

Precise calculation of neutralino relic density in the minimal supergravity model^a

Takeshi Nihei

Department of Physics, Lancaster University, Lancaster LA1 4YB, England, UK

We study precise calculation of neutralino relic density in the minimal supergravity model. We compare the exact formula for the thermal average of the neutralino annihilation cross section times relative velocity with the expansion formula in terms of the temperature, including all the contributions to neutralino annihilation cross section. We confirm that the expansion formula fails badly near s-channel poles. We show that the expansion method causes 5-10 % error even far away from the poles.

1 Introduction

In recent years, observations of cosmic microwave background radiation have been providing experimental values for cosmological parameters with some accuracy. Current experimental bound on the fractional energy density of cold dark matter is [2, 3]

$$\Omega_{\text{CDM}}h^2 = 0.1 - 0.3, \quad (1)$$

where $h \approx 0.7$ is the parameter in the Hubble constant $H_0 = 100 h \text{ km/sec/Mpc}$ [4]. This bound (1) is expected to be improved in the near future, so precise calculation of the relic density becomes important.

Particle physics should provide a particle-theoretical explanation for dark matter. The minimal supergravity model [5] is one of the most promising candidate for new physics beyond the standard model. In this model, a discrete symmetry, so-called R-parity, is introduced to avoid rapid proton decay. One of the consequences of introducing the R-parity is that the lightest superparticle (LSP) is stable, and the LSP becomes a good candidate for cold dark matter [6]. The LSP in this model is mostly the lightest neutralino χ which is a mass eigenstate given by a linear combination of neutral gauginos and Higgsinos

$$\chi = N_{11}\tilde{B} + N_{12}\tilde{W}^3 + N_{13}\tilde{H}_1^0 + N_{14}\tilde{H}_2^0. \quad (2)$$

In general, supersymmetric models have a huge number of unknown parameters. However, the minimal supergravity model has only a small number of parameters, so it has reasonable predictive power. There are five unknown

^aThis talk is based on the work [1].

parameters in this model

$$m_0, m_{1/2}, A, \tan\beta, \text{sgn}(\mu), \quad (3)$$

where m_0 , $m_{1/2}$ and A represent a common scalar mass, a common gaugino mass, and a common trilinear scalar coupling, respectively. They parametrize soft supersymmetry breaking terms at the GUT scale $\approx 2 \times 10^{16}$ GeV. $\tan\beta$ is the ratio of vacuum expectation values of the two neutral Higgs fields. μ denotes the Higgs mixing mass parameter. In the case of the minimal supergravity model, the absolute value of μ is determined from the condition for consistent radiative electroweak symmetry breaking, and only the sign is a free parameter. In this work, we assume that there are no CP violating phases in these parameters (3) for simplicity.

2 Calculation of the relic density

In this section, we first briefly review the standard calculation of the neutralino relic density [7] in the minimal supergravity model. After that, we explain what is necessary to calculate it precisely.

We evaluate the relic density at present, starting from thermal equilibrium in the early universe. The time evolution of the neutralino number density in the expanding universe is described by the Boltzmann equation

$$\frac{dn_\chi}{dt} + 3Hn_\chi = -\langle\sigma v_{\text{Møll}}\rangle (n_\chi^2 - n_\chi^{\text{eq}2}), \quad (4)$$

where H is the Hubble expansion rate. n_χ describes the actual number density of the neutralino, while n_χ^{eq} is the number density which the neutralino would have in thermal equilibrium. σ denotes the cross section of the neutralino pair annihilation into ordinary particles. $v_{\text{Møll}}$ is so-called Møller velocity which can be identified as the relative velocity between the two neutralinos. $\langle\sigma v_{\text{Møll}}\rangle$ represents the thermal average of $\sigma v_{\text{Møll}}$.

In the early universe, the neutralino is in thermal equilibrium $n_\chi = n_\chi^{\text{eq}}$. As the universe expands, the neutralino annihilation process freezes out, and after that the number of the neutralinos in a comoving volume remains constant.

In the annihilation cross section σ in eq. (4), there are a lot of final states which contribute: $\chi\chi \rightarrow f\bar{f}, hh, WW, ZZ, Zh$, etc. Among these final states, fermion pairs $f\bar{f}$ usually give dominant contributions.

Using an approximate solution to the Boltzmann equation (4), the relic density $\rho_\chi = m_\chi n_\chi$ at present is given by

$$\rho_\chi = 1.66 \frac{1}{M_{\text{Pl}}} \left(\frac{T_\chi}{T_\gamma}\right)^3 T_\gamma^3 \sqrt{g_*} \frac{1}{\int_0^{x_F} dx \langle\sigma v_{\text{Møll}}\rangle}, \quad (5)$$

where $x = T/m_\chi$ is a temperature of the neutralino normalized by its mass. T_χ and T_γ are the present temperatures of the neutralino and the photon, respectively. The suppression factor $(T_\chi/T_\gamma)^3 \approx 1/20$ follows from the entropy conservation in a comoving volume [8]. M_{Pl} denotes the Planck mass. $x_F \approx 1/20$ is the value of x at freeze-out, and is obtained by solving the following equation iteratively:

$$x_F^{-1} = \ln \left(\frac{m_\chi}{2\pi^3} \sqrt{\frac{45}{2g_* G_N}} \langle \sigma v_{\text{Mol}} \rangle_{x_F} x_F^{1/2} \right), \quad (6)$$

where G_N is the Newton's constant, and g_* represents the effective number of degrees of freedom at freeze-out.

The relativistic formula [9] for thermal average in eq. (4) can be written as an integration over one variable [10]

$$\langle \sigma v_{\text{Mol}} \rangle = \frac{1}{8m_\chi^4 T K_2^2(m_\chi/T)} \int_{4m_\chi^2}^{\infty} ds \sigma(s) (s - 4m_\chi^2) \sqrt{s} K_1 \left(\frac{\sqrt{s}}{T} \right), \quad (7)$$

where K_i ($i = 1, 2$) are the modified Bessel functions. The cross section $\sigma(s)$ is a complicated function of s in general, so we have to evaluate the above integration numerically to calculate the thermal average.

If the normalized temperature x is small enough, we may be able to use an expansion formula in terms of x for the thermal average (7)

$$\langle \sigma v_{\text{Mol}} \rangle = a + bx. \quad (8)$$

This expansion, neglecting the higher order of x , is widely used in literatures. In the case that the neutralino is the LSP, the a coefficient for a fermion pair production is proportional to the fermion mass due to the Majorana nature of the neutralino. On the other hand the b coefficient for the same final state includes a contribution which is not proportional to the fermion mass, so the b coefficient is much larger than the corresponding a coefficient for each fermionic final state: $a \ll b$ [11].

In order to calculate the relic density precisely enough, we have to take into account the following items:

- (i) all the contributions to the annihilation cross section
- (ii) the exact formula for the thermal average
- (iii) solving the Boltzmann equation exactly
- (iv) coannihilation (This becomes important when the mass of the next LSP is close to the LSP mass [12–15].)

In this work, however, we concentrate on (i) and (ii) to compare the expansion formula with the exact one, and we don't take into account (iii) and (iv) for simplicity. Namely, we use the approximate solution (5) to the Boltzmann equation, and we neglect coannihilation effects.

We have derived analytic expressions for the exact annihilation cross section and have obtained a and b coefficients analytically for every contribution including interference terms. These interference terms are neglected in most literatures, but we found that they can give significant contributions in some cases. Some of the analytic expressions can be found in literatures for both the exact cross section [16, 17] and the expansion coefficients [18, 19].

3 Thermal average — exact formula vs. expansion

Let us see the rough behavior of the integrand in eq. (7). In the case of interest, the argument of the function K_1 is much larger than unity, since $T \lesssim m_\chi/20$ and $\sqrt{s} \geq 2m_\chi$. Therefore the thermal average can be written as a convolution of the cross section with a function which decays exponentially:

$$\langle \sigma v_{\text{Mø}} \rangle \approx \int_{4m_\chi^2}^{\infty} ds \sigma(s) F(s), \quad (9)$$

where the function $F(s)$ has an exponential suppression factor as

$$F(s) \propto e^{-\sqrt{s}/T}. \quad (10)$$

Naively, it seems that the expansion should converge quickly, since the function $F(s)$ in eq. (10) decays exponentially as s increases [9]. However this is not always true. It is known that the expansion method fails badly when the annihilation cross section changes rapidly with s [10, 12, 16]. This happens, e.g. near s-channel poles and thresholds of new channels. In the following we compare the expansion result with the exact one, including all the contributions to the annihilation cross section.

4 Numerical results

The spectrum and the couplings in the minimal supergravity model at the weak scale are calculated by solving renormalization group equations with boundary conditions at the GUT scale and implementing radiative electroweak symmetry breaking. In this analysis, we use an existing code ‘‘SUSPECT’’ [20] to calculate the spectrum and the couplings.

In the following, we present the results of our calculation. Fig. 1 shows the integration of the thermal average $\int_0^{x_F} dx \langle \sigma v_{\text{Mø}} \rangle$ as a function of $m_{1/2}$

for $\tan\beta = 2$, $m_0 = 200$ GeV, $A = 0$, $\mu > 0$. Note that the relic density in eq. (5) is proportional to the inverse of this integration. The solid line and the dashed line represent the exact result and the expansion result, respectively.

We have plotted the total contributions and the individual contributions for relevant final states. The exact results show similar behaviors with those in a previous analysis [21].

There are two peaks in the total contributions. One is from the Z boson contribution, and it takes place when $2m_\chi \approx m_Z$ is satisfied. The other is from the lightest Higgs (h) contribution, and it happens when $2m_\chi \approx m_h$. Around the poles, we see huge difference between the exact result and the expansion. Away from the poles, the difference is not so huge.

We plot the relic density vs. $m_{1/2}$ in Fig. 2 (a) for the same parameters as those in Fig. 1. In the region of the poles, we see a dip of the relic density. Away from the poles, the relic density is too large to satisfy the experimental constraint (1).

In Fig. 2 (b), we plot the ratio $\Omega_{\text{expansion}}/\Omega_{\text{exact}}$, where Ω_{exact} ($\Omega_{\text{expansion}}$) denotes the relic density calculated with the exact (expansion) formula for the thermal average. In the pole regions, the expansion is quite different from the exact one by a large factor [16]. Also we find a difference of about 5 % in this ratio even far away from the pole.

In a very large $\tan\beta$ case, the result has a different feature. In Fig. 3 (a) and (b), we show similar results for $\tan\beta = 50$, $m_0 = 600$ GeV, $A = 0$, $\mu > 0$. The relic density is small due to enhancements of the pseudoscalar Higgs exchange contribution and the heavier neutral Higgs exchange contribution in the $b\bar{b}$ final state for a large $\tan\beta$. There are two reasons for these enhancements. First, couplings of the pseudoscalar Higgs and the heavier neutral Higgs to the bottom quark become large for a large $\tan\beta$. Secondly, masses of heavy Higgses become smaller in a large $\tan\beta$ region. Because of these enhancements in the annihilation cross section, the relic density in Fig. 3 (a) becomes small enough to satisfy the experimental constraint (1) for a wide region of 600 GeV $< m_{1/2} < 800$ GeV. As for the ratio of the expansion result to the exact one in Fig. 3 (b), we see a difference more than 10 % for 600 GeV $< m_{1/2} < 800$ GeV. Note that we find this relatively large difference in the interesting region where the relic density satisfies the experimental constraint (1).

We show a contour plot for the quantity $2m_\chi - m_A$ for $\tan\beta = 50$, $A = 0$ and $\mu > 0$ in Fig. 4, where m_A denotes the pseudoscalar Higgs mass. Along the thin solid line, this quantity vanishes so that there are enhancements in the annihilation cross section from the pseudoscalar Higgs pole contribution and the heavier neutral Higgs pole contribution through the $b\bar{b}$ final state. Fig. 4 shows that the region 600 GeV $< m_{1/2} < 800$ GeV in Fig. 3 (b), where the

deviation of $\Omega_{\text{expansion}}$ from Ω_{exact} is about 10 %, differs from the pole region (i.e. the zero of the quantity $2m_\chi - m_A$) in m_0 by about 150 GeV. Despite of this difference, we still have a sizable error of 10 % in the expansion result, as we have seen in Fig. 3 (b).

In Fig. 2 and Fig. 3, we find 5-10 % difference even away from the pole. Thus the expansion never succeeds to approximate the exact result within the accuracy of 5 %. This implies that the coefficient of the next order cx^2 in the expansion (8) has the same order with the b coefficient $c/b \approx O(1)$.

5 Conclusions

We have presented results of precise calculation of neutralino relic density in the minimal supergravity model. We have calculated all the contributions to neutralino annihilation cross section analytically. We have compared the exact formula for the thermal average of the annihilation cross section times relative velocity with the expansion formula in terms of the temperature. We have confirmed that the expansion formula fails badly near s-channel poles. We have shown that the expansion method causes 5-10 % error even far away from the poles.

Acknowledgments

The author was supported in part by PPARC grant PPA/G/S/1998/00646.

References

1. T. Nihei, L. Roszkowski and R. Ruiz, in preparation.
2. P. de Bernardis *et.al.*, *Nature* **404**, 955 (2000).
3. A. Balbi *et.al.*, astro-ph/0005124.
4. W. Freedman, *Phys. Rep.* **333**, 13 (2000).
5. For reviews on the minimal supergravity model, see for instance, H.P. Nilles, *Phys. Rep.* **110**, 1 (1984); P. Nath, R. Arnowitt and A.H. Chamseddine, *Applied N = 1 Supergravity*, World Scientific, Singapore (1984).
6. J. Ellis, J.S. Hagelin, D.V. Nanopoulos, K.A. Olive and M. Srednicki, *Nucl. Phys. B* **238**, 453 (1984).
7. For reviews on calculations of the relic density, see for instance, E.W. Kolb and M.S. Turner, *The Early Universe*, Addison-Wesley (1990); G. Jungman, M. Kamionkowski and K. Griest, *Phys. Rep.* **267**, 195 (1996).
8. K.A. Olive, D. Schramm and G. Steigman, *Nucl. Phys. B* **180**, 497 (1981).

9. M. Srednicki, R. Watkins and K.A. Olive, *Nucl. Phys. B* **310**, 693 (1988).
10. P. Gondolo and G. Gelmini, *Nucl. Phys. B* **360**, 145 (1991).
11. H. Goldberg, *Phys. Rev. Lett.* **50**, 1419 (1983).
12. K. Griest and D. Seckel, *Phys. Rev. D* **43**, 3191 (1991).
13. S. Mizuta and M. Yamaguchi, *Phys. Lett. B* **298**, 120 (1993).
14. J. Edsjö and P. Gondolo, *Phys. Rev. D* **56**, 1879 (1997).
15. J. Ellis, T. Falk, K.A. Olive and M. Srednicki, *Astropart. Phys.* **13**, 181 (2000).
16. J.L. Lopez, D.V. Nanopoulos and K. Yuan, *Phys. Rev. D* **48**, 2766 (1993).
17. K. Griest, M. Kamionkowski, and M.S. Turner, *Phys. Rev. D* **41**, 3565 (1990).
18. J. Ellis, L. Roszkowski and Z. Lalak, *Phys. Lett. B* **245**, 545 (1990); K.A. Olive and M. Srednicki, *Nucl. Phys. B* **355**, 208 (1991).
19. M. Drees and M. Nojiri, *Phys. Rev. D* **47**, 376 (1993).
20. A. Djouadi, J.-L. Kneur and G. Moultaka, the code available on the web at <http://www.lpm.univ-montp2.fr:7082/~kneur/suspect.html>.
21. H. Baer and M. Brhlik, *Phys. Rev. D* **53**, 597 (1996).

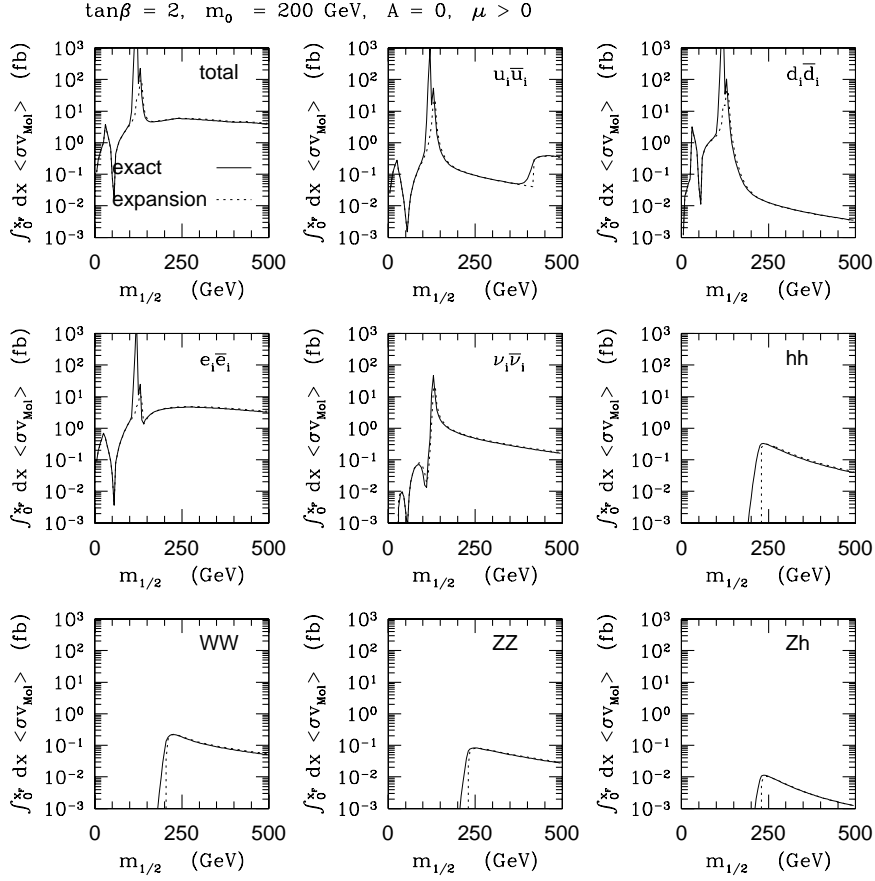


Figure 1: Integration of the thermal average $\int_0^{x_F} dx \langle \sigma v_{\text{Mol}} \rangle$ as a function of $m_{1/2}$ for $\tan\beta = 2, m_0 = 200 \text{ GeV}, A = 0, \mu > 0$.

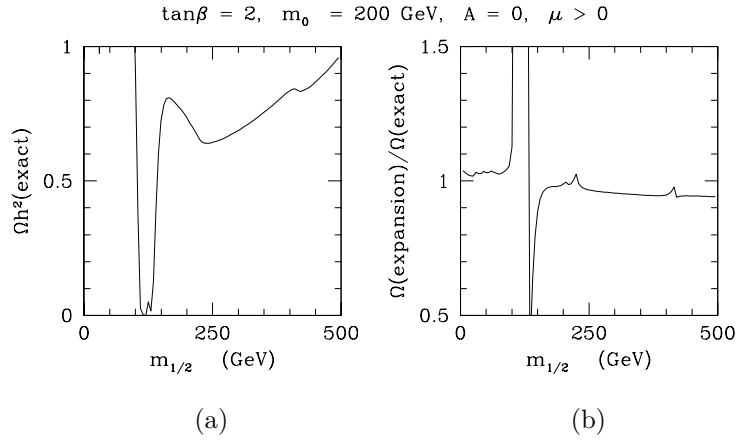


Figure 2: The relic density Ωh^2 (a) and the ratio $\Omega_{\text{expansion}}/\Omega_{\text{exact}}$ (b) for $\tan\beta = 2, m_0 = 200 \text{ GeV}, A = 0, \mu > 0$.

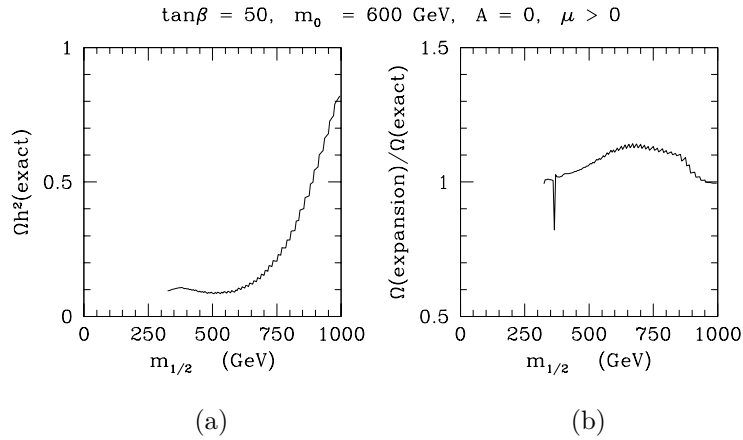


Figure 3: Similar results to Fig. 2 for $\tan\beta = 50, m_0 = 600 \text{ GeV}, A = 0, \mu > 0$.

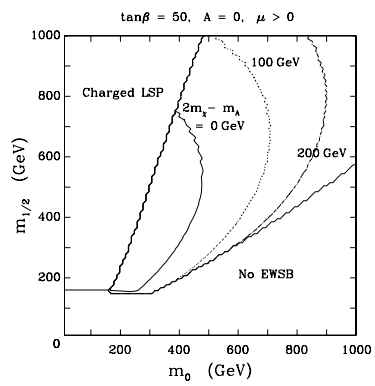


Figure 4: A contour plot of $2m_\chi - m_A$ in the m_0 - $m_{1/2}$ plane for $\tan\beta = 50$, $A = 0$ and $\mu > 0$. The region 'Charged LSP' is excluded because the lighter stau is the LSP in this region. In the region 'No EWSB', the electroweak symmetry breaking does not occur.